

Mean surface meteorological parameter characterization at Kavaratti, Lakshadweep Island, South-East Arabian Sea

Vijay Kumar^{1*}, Prakash Mehra¹, Balakrishnan Nair², Yogesh Agarvadekar¹, Ryan Luis¹, Devika Ghatge¹,
Shane Lobo¹ and Bharat Harmalkar¹

¹CSIR-National Institute of Oceanography, Dona Paula, Goa-403004

²ESSO-Indian National Centre for Ocean Information Services, Hyderabad, India - 500 090

*[Email: kvkumar@nio.org]

Received 21 August 2013; revised 30 October 2013

Soon after the south-west monsoon, mean surface meteorological parameters at the Kavaratti Island begin to change. Wind, which was south-west in direction during the monsoon period, turns to north-north and eventually to north-east direction with lesser intensity. Monthly mean wind speed in October was $\sim 2 \text{ ms}^{-1}$ while in July it was $\sim 7 \text{ ms}^{-1}$. Monthly mean surface air pressure in October was $\sim 1008 \text{ hPa}$ as against $\sim 1007 \text{ hPa}$ in July. Surface air-temperature and relative humidity also exhibited similar variability. Monthly mean air temperature and humidity in October were $\sim 28^\circ\text{C}$, and $\sim 76\%$ respectively, while in July $\sim 26^\circ\text{C}$, and $\sim 87\%$ respectively were recorded. In general, wind was predominantly in the north/north-westerly direction throughout the year, except June-July during which a west/south-westerly winds was observed. Minimum atmospheric pressure occurs during June-July (southwest monsoon period) and the maximum during December-January (northeast monsoon period). Air temperature demonstrates steady increase from January to May before descending to minimum during July-August. During the observational period (2009) inverse relationships between barometric pressure and air-temperature was observed. Similar relationship between relative humidity and air-temperature was also noticed.

[Keywords: Real time meteorological parameters, surface wind, air-temperature, atmospheric-pressure, relative humidity, specific humidity]

Introduction

Meteorological parameters are one of the key inputs to the numerical models in a study of atmospheric circulation, weather system and pollutant transport. Measuring surface meteorological parameters in real time is useful to many communities such as oceanographers and environmentalists, navigators, harbour managers and disaster management agencies. The CSIR-National Institute of Oceanography (hereafter CSIR-NIO) has developed real/near-real time Internet accessible systems for monitoring of coastal sea level, and surface meteorological parameters and can be accessed through <http://inet.nio.org>. These systems were primarily developed for collecting data for in-house scientific investigations. However, such systems are also useful for validating numerical models, real-time weather information and operational purposes in ports and harbours. The present study area, (i.e., Kavaratti Island in the Lakshadweep Archipelago) is located in the South East of the Arabian Sea (10.34°N , 72.38°E) approximately 400 km from the west coast of India. The length and the width of the island are $\sim 5.8 \text{ km}$ and $\sim 1.6 \text{ km}$ respectively. It is surrounded by a lagoon

having an area of ~ 5 square km and stretching in length to $\sim 6 \text{ km}$. An Autonomous Weather Station (hereafter NIO-AWS), designed and developed by the Marine Instrumentation group of CSIR-NIO, Goa, was used for this study. One of the key usages of this data was to provide latest wind and barometric-pressure information to the air-port manager, Kavaratti, while planning aircraft services. In this manuscript, we attempt to describe surface meteorological conditions over Kavaratti Island. Section 2 briefly describes observational setup, section 3 provides analysis and interpretation, followed by results and discussions in section 4 and conclusions are presented in section 5.

Materials and Methods

Observational setup and data collection

NIO-AWS was installed on the terrace of the Port Control Tower (PCT) for surface meteorological observations (Fig.1). The PCT was chosen for the observational setup as it is the tallest building on Kavaratti Island ($\sim 10\text{m}$) and located close to the seashore (the horizontal distance between the PCT and the sea water line is within 100m). The PCT is

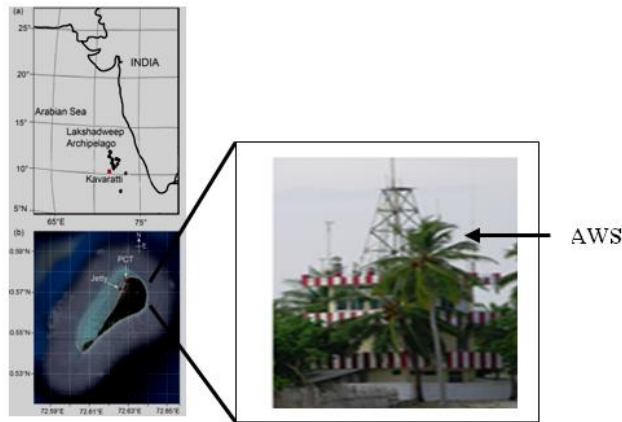


Fig.1—NIO-AWS installation on the terrace of the Port Control Tower at Kavaratti Island

surrounded by coconut trees and residential shelters. However, the sea facing area of the PCT is free from any obstructions. The terrace of the PCT is a horizontal levelled surface on which Radio Frequency (RF) towers and antennae are fixed for offshore ship, rescue, and evacuation communications. The NIO-AWS was installed on a cement platform (dimension $\sim 2' \times 2' \times 1'$) above the terrace surface level using a Galvanized Iron (GI) mast of 1.5" diameter on which sensors were mounted. The mast height was $\sim 3\text{m}$ and sensor level was $\sim 36\text{m}$ above the mean sea level. Observed wind was converted to logarithmic wind (U_{10}) following the World Meteorological Organization (WMO) convention. The position of the anemometer was almost at the same level as the pinnacle of the coconut tree. The NIO-AWS was powered from a 12-Volt battery kept in the PCT room. It measures wind speed & direction, wind gust, barometric pressure, solar radiation, air temperature, and relative humidity at 10-min intervals. Each parameter was sampled at an interval of 10seconds and each measurement, except gust (i.e., the largest wind speed amongst an ensemble of 60 samples that were measured during the 10-minute sampling span), was an average over 10 minutes (i.e., average of 60 samples). Wind was vector-averaged.

The technical details of the NIO-AWS sensors are given in Table 1. The Internet access to the NIO-AWS network was implemented via cellular GPRS¹ and can be accessed through <http://inet.nio.org>. A dedicated server at CSIR-NIO, (Goa) stores the real/near-real time data and displays it on Internet for

Table 1— Technical detail of sensors used for surface meteorological observations

Surface meteorological parameters	Sensors	Manufacturer	Range	Accuracy
Wind speed & direction	Four-blade helecoid propeller (speed) and light weight vane & precision potentiometer (direction)	RM Young, USA	0-100 ms^{-1} 0-360°	$\pm 0.3\text{ms}^{-1}$ $\pm 0.3^\circ$
Temperature	Thermistor	YSI, USA	0-45°C	$\pm 0.15^\circ\text{C}$
Barometric pressure	Temperature-compensated piezoresistive strain-gauge pressure transducer	Honeywell, USA	500-1200 hPa	$\pm 0.4\text{ hPa}$
Humidity	Polymer capacitor sensor	Rotronic, USA	0-100 % RH	$\pm 3\% \text{ RH}$
Solar radiation	Silicon photodiode with wide spectral response	Licor, USA	0-300 mWcm^{-2}	$\pm 5\%$

the public and stakeholders (Fig.2). In addition, data were also stored in a dedicated on-board data logger of the NIO-AWS.

Data analysis and interpretation

Although surface meteorological parameters at Kavaratti Island were collected over a year, data are analyzed for the year 2009 and results are presented in the following sub sections:

Wind and gust

The observed wind circulation over a year provides an indication of the typical annual cycle in the eastern Arabian Sea and the west coast of the Indian Peninsula. We examine below the features of the wind field beginning from January. January-February months fall under the winter season during which both wind gust (Fig.3) and 10-min average wind speed (Fig. 4) at Kavaratti Island were $\sim 5\text{-}7\text{ ms}^{-1}$. The monthly-mean wind gust peak in July was $\sim 6.5\text{ ms}^{-1}$, indicating that the wind in this region is the most

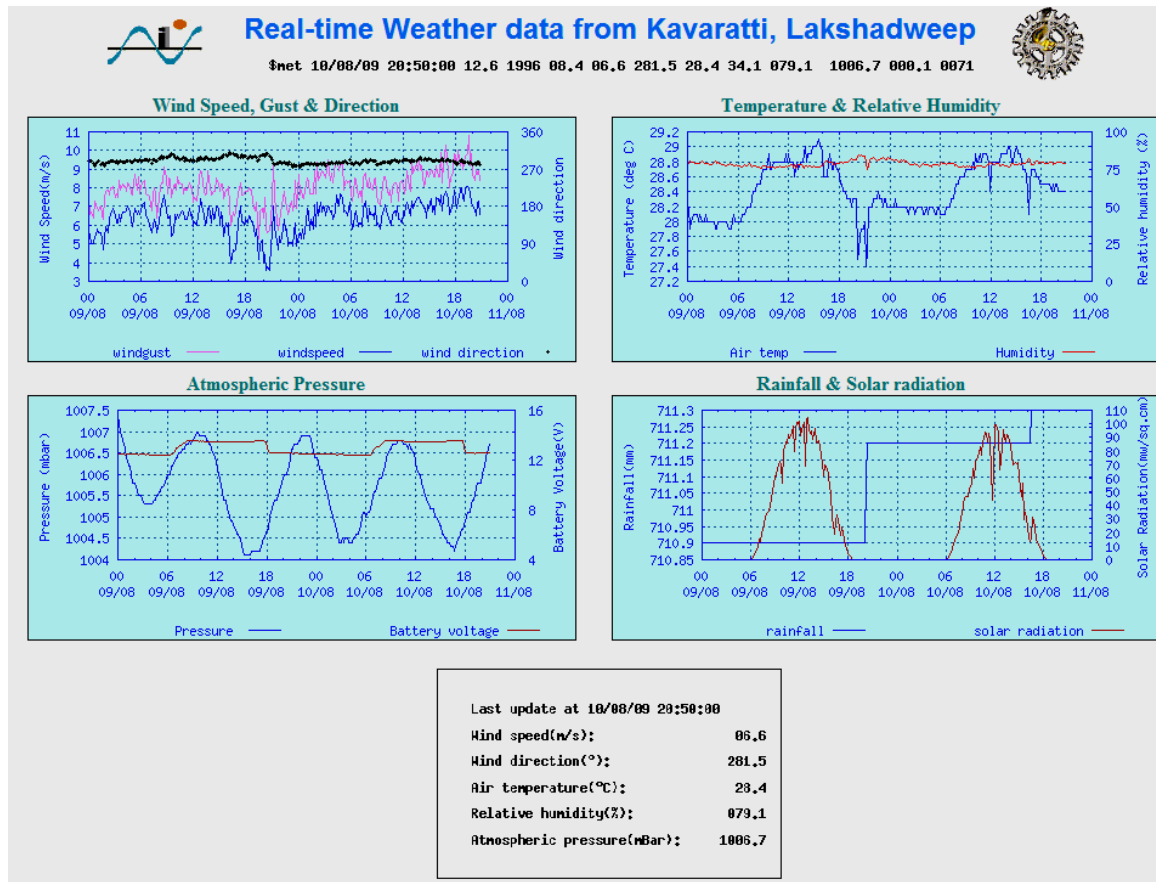


Fig. 2—Real/near-real time Internet display of the NIO-AWS data

unsteady in July. In contrast, the monthly-mean wind speed peaked in August at $\sim 4.25 \text{ ms}^{-1}$ indicating that

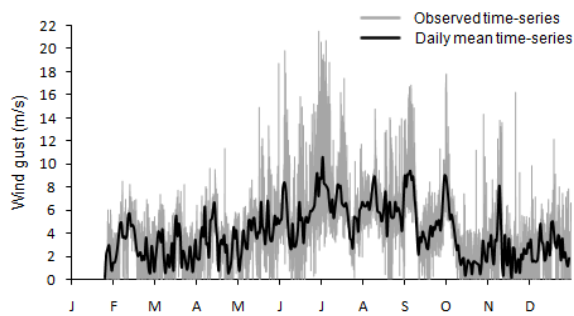


Fig. 3—Surface wind gust time-series data for the year 2009 collected from Kavaratti Island. Daily-mean time-series is superimposed on the observed time-series data sampled at 10-minute intervals

the largest steady wind occurs in August. The wind rose constructed based on the data collected from Kavaratti Island is shown in (Fig.5). These figures provide an indication of the general characteristics of the wind field (both speed and direction) in the Lakshadweep Archipelago region. The wind rose

shows that during the winter season the wind direction flips from north/north-easterly to predominantly northerly. During pre-monsoon (March-May), wind gust and speed continues to remain at $\sim 5-7 \text{ ms}^{-1}$. However, the wind direction tends to be confined within the north-west sector (i.e., north-westerly wind flow occurs during the pre-monsoon).

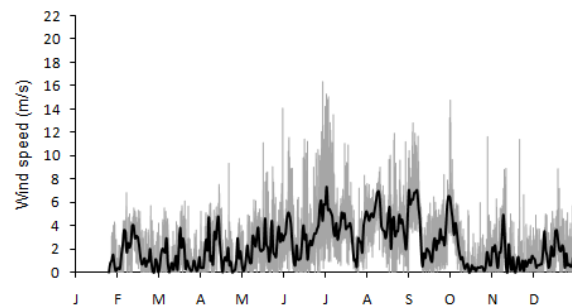


Fig. 4—Ten-minute averaged surface wind time-series data for the year 2009 collected from Kavaratti Island. Daily-mean time-series is superimposed on the observed time-series data sampled at 10-minute intervals

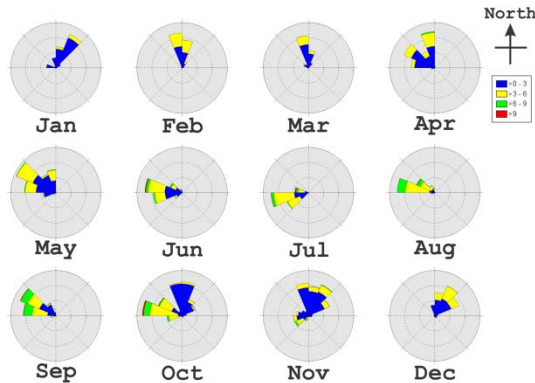


Fig. 5—Wind rose for the year 2009 based on the data collected from Kavaratti Island, providing an indication of the general characteristics of the wind field in the Lakshadweep Islands region.

The Lakshadweep Archipelago region falls under the influence of both South-West (SW) monsoon (June-September period) and North-East (NE) monsoon (October-December period). The cyclonic storm “Phyan”², which swept along the Eastern Arabian Sea in November 2009, provided an extra boost to the wind field in this region. The wind during the NE monsoon period was primarily north-easterly. However, north-westerly winds have also been occasionally observed here in the month of October. The SW monsoon period exhibits the observed maximum wind gust (up to $\sim 22 \text{ ms}^{-1}$) as well as the 10-min averaged wind speed (up to $\sim 17 \text{ ms}^{-1}$). During this season, the wind was primarily westerly. However, it occasionally vacillates between north-westerly and south-westerly.

Atmospheric temperature

Our measurements of the surface air temperature (AT) at Kavaratti Island (Fig. 6) indicate that this parameter in the Lakshadweep Archipelago region exhibits strong seasonal variability. AT undergoes diurnal day-night variability. In January-February, the measured diurnal variability in this region was in the range of $\sim 3\text{-}4^\circ\text{C}$. Whereas the daily-mean AT in January-February was $\sim 27\text{-}28^\circ\text{C}$, it gradually increases and ultimately reaches a peak value of $\sim 30^\circ\text{C}$ in May-June. Subsequently, with the onset of the SW monsoon, the temperature starts falling and the daily-mean temperature dips to $\sim 26^\circ\text{C}$ in July.

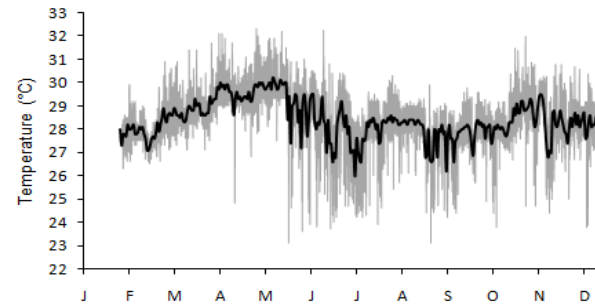


Fig. 6—Ten-minutes averaged atmospheric temperature time-series data for the year 2009 collected from Kavaratti Island. Daily-mean time-series is superimposed on the observed time-series data sampled at 10-minute intervals.

Hereafter, the temperature starts gradually rising and touches $\sim 29.5^\circ\text{C}$ in November. However, the cyclonic storm “Phyon” gave rise to a rapid drop in the daily-mean AT (by $\sim 3^\circ\text{C}$). With the decay of the storm intensity, the temperature bounced up by $\sim 2^\circ\text{C}$ and continued to maintain more or less this level until it dropped again by the peak winter. Measurement provides evident that whereas the pre-monsoon months (March-May) exhibits the annual maximum air-temperature ($\sim 30^\circ\text{C}$), the SW monsoon months exhibits the annual minimum air-temperature ($\sim 28^\circ\text{C}$). A well-marked intermediate temperature ($\sim 28.25^\circ\text{C}$) was observed during October-January months.

Atmospheric pressure

The atmosphere is composed primarily of air and moisture; and because of it being fluid, atmospheric pressure undergoes a semi-diurnal variability under the influence of time-varying forces exerted by the Sun and the Moon as well as the rotation of the Earth about its own axis; together with the fortnightly vacillation of the Earth about the plane of motion of the planets (this is akin to the semi-diurnal tides in large water bodies such as oceans, seas, and lakes). During April-May, the Indian subcontinent gets huge amount of heat due to solar insolation, the surface pressure decreases and shallow trough ($\sim 2\text{-}3 \text{ km}$ from surface) appears over the heated landmass³⁻⁴. The Lakshadweep Archipelago region (like the west coast of India) exhibits a distinctly clear seasonal variability in atmospheric pressure (AP) (See Fig. 7). It reveals gradual shift from lower pressure to higher pressure

and then again low. During winter (January-February) AP was ~1009 hPa. However, it subsequently starts dropping and reaches the annual low (~1005hPa) by May (peak summer).

With the atmospheric cooling resulting from the south-west monsoon rainfall, AP starts rising from June and continues to do so until October during which it was ~1008 hPa. However, the storm Phyon forced a steep drop in AP down to ~998 hPa. With the weakening of the storm, AP starts rising again, exceeding 1008 hPa by December. When several atmospheric parameters contribute to the overall climatology, it may be worthwhile to examine the inter-relationships among them. One such inter-relationship that is observed was an inverse relationship between monthly-mean AP and AT. This is quite understandable because the expansion of air under increasing AT reduces air density, thereby reducing the AP.

Relative humidity

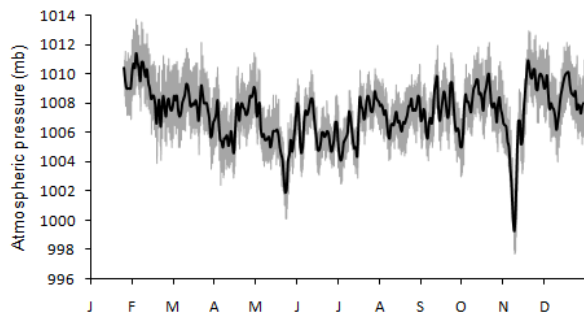


Fig. 7—Ten-minutes averaged atmospheric pressure time-series data for the year 2009 collected from Kavaratti Island. Daily-mean time-series is superimposed on the observed time-series data sampled at 10-minute intervals.

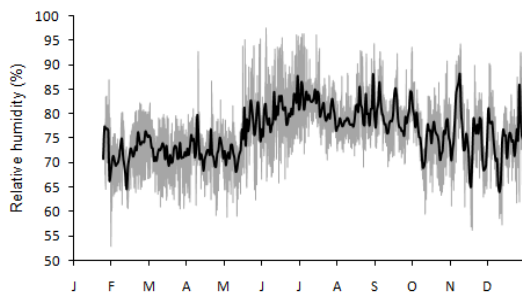


Fig. 8—Ten-minutes averaged relative humidity time-series data for the year 2009 collected from Kavaratti Island. Daily-mean time-series is superimposed on the observed time-series data sampled at 10-minute intervals

Humidity is an important surface-meteorological parameter for climatological study. Our measurements (Fig. 8) indicate that February-May exhibit relative humidity (RH) in the range of ~65-80%, during which there was little rainfall and the annual atmospheric temperature was large. The onset of south-west monsoon in June causes a substantial increase in RH, with 10-min averaged value in the range of ~65-98% and daily-mean value in the range of ~80-85%. The peak RH occurs in July. Subsequently, the observed RH reveals a decreasing trend and rises again during the northeast monsoon rainfall, but it was considerably less than that during the south-west monsoon season. The monthly-mean RH reveals a clear indication of the annual dominance of RH in July.

The specific humidity (i.e., the ratio of mass of water vapour to the total mass of the air) is related to the atmospheric density. During the year 2009 specific humidity was estimated using the relationship⁵⁻⁷

$$q = \frac{\rho_v}{\rho} = \frac{0.622e}{(p-0.378e)} \quad \dots (1)$$

$$e = 6.112 \exp\left(\frac{17.67t}{t+243.5}\right) \quad \dots (2)$$

Where, q is specific humidity (kg kg⁻¹), ρ = ρ_a+ ρ_v is the density of the moist air, ρ_a is dry air density (kgm⁻³), ρ_v is water vapour density (kgm⁻³), e is vapour pressure (mb), p is barometric pressure (mb), t is temperature (°C) and RH is relative humidity. The vapour pressure (e) is always expressed with respect to water and has maximum concentration near the earth's surface⁷. It decreases with increasing height from the surface, depending more on temperature and weakly on pressure.

The seasonal variations in specific humidity were small as compared to the air-temperature variations (Fig. 9). Monthly mean specific humidity during December-February was $\sim 17 \text{ gkg}^{-1}$ while during June-September $\sim 19 \text{ gkg}^{-1}$ was observed.

Results and Discussion

Land-sea heat contrast over southern Asia sets up an atmospheric pressure gradient during December-March, which results in surface wind flowing southward over Arabian Sea (see Fig.5). During this period, there is also a weak equatorial trough in the south east Arabian Sea and across the south peninsula of India^{4,8-9}. Consequently, cold air masses from the higher latitude flow towards the Indian peninsula and surrounding seas thereby reducing the temperature gradients between land and sea. As a result, the NE monsoon is weaker than the SW monsoon. Our observations suggest that during the NE monsoon winds were, generally, less than 5 ms^{-1} and were not as strong as during the SW monsoon. More variability was seen than during the SW monsoon and most of this variability could be related to the intrusion of a polar jet trough⁴. The fluctuations in the wind were typically associated with low temperature (e.g., in December 24°C) and with lesser humidity. In general, wind minima were noticed around 05-h, 13-h, 15-h, and 21-h and maxima were around 08-h, 18-h, and 20-h. However, there have been considerable variations in period and time from day to day observations. Humidity has shown a diurnal pattern with minima around 13-h and maxima around 03-h. The AP showed a gradual shift from high pressure to lower pressure from mid January/February to May. Typical one year pressure records revealed the appearance of an inverted dome-bell shape curved at the Lakshadweep Islands (Fig.7). Shift in wind directions from NE to North-West (NW) (e.g., during February-March) could be linked to temporarily regional AP imbalance from high latitude disturbances that extend to the Arabian Sea.

As the sun moves in the Northern hemisphere, there is rapid increase in incoming solar radiation which results in rise in surface air-temperature (e.g., during February-April). Consequently, the continental high pressure zone changes to a low

pressure area. Simultaneously, a weaker near-equatorial trough, which exists during the NE monsoon, replaces the low level central Arabian Sea high pressure. Because of the change in the flow circulation pattern light and variable winds prevail in the Arabian Sea region³. In April, daily mean winds were measured $\sim 1.5 \text{ ms}^{-1}$. By late May, surface air pressures had changed direction from the December-March pattern and winds were more dominant in NW/SW directions. During this period, average wind speeds were $< 6 \text{ ms}^{-1}$, and were occasionally over 8 ms^{-1} .

Although south westerly winds may appear weak during April-May, the SW monsoon generally starts with high turbulent wind and intense precipitations in the cross equatorial region. As strengthened south westerly winds progress towards the northeast across the Arabian Sea, an enhanced convective process sweeps towards the west coast of India which is normally associated with onset vortex, e.g.,¹⁰⁻¹¹. In early June, south westerly winds were observed to be blowing from SW-NW directions and subsequently became more intense and focused in SW direction in July (Fig.5). During the onset of the SW monsoon, wind speeds were initially high ($> 5 \text{ ms}^{-1}$), then became low ($< 2 \text{ ms}^{-1}$) in early June for few days and rose again to high ($> 10 \text{ ms}^{-1}$) in the last week of June. The wind speed and air pressure has shown good correlation (e.g., when wind speed was $\sim 15 \text{ ms}^{-1}$ AP was $\sim 1002 \text{ hPa}$ and when wind speed was $\sim 0.4 \text{ ms}^{-1}$ AP recorded $\sim 1009 \text{ hPa}$). The total pressure gradients in the study area were relatively constant from day to day observations, however, seasonal distributions were significantly variable, contributing to strong and weak winds. At either end of the monsoon period (i.e., June and September) winds were not consistent with SW

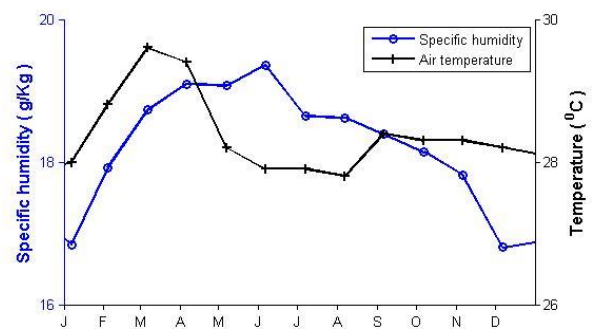


Fig. 9—Monthly-mean specific humidity and atmospheric temperature time-series data for the year 2009 collected from Kavaratti Island

direction but were oscillating in NW and SW directions. The relative humidity during the SW monsoon was high (~96%) and increased progressively from June. The variability in RH was less during this period. The AT has also shown less variability (more or less around 27°C); however seasonal mean was ~28°C. Seasonal mean wind speed and direction were ~6 ms⁻¹ and 280° respectively. While seasonal mean humidity and AP were ~80% and ~1007 hPa respectively.

By mid September the sun starts retreating towards the south. As a result, during October-November, the amount of insolation (i.e., incident solar radiations) received over the northern hemisphere decreases rapidly causing low heat over the continental landmasses. As the land masses cool down, a high air pressure builds up over the land resulting in air pressure gradient which allows the winds to flow from a high air pressure zone to a lower air pressure area. Changes in wind fields from large scale southwesterly-northwesterly flow to north easterly flow are seen in early October (Fig. 5). In October, wind speeds were light (< 5 ms⁻¹) but by November light to moderate north easterly winds prevailed over the entire region of Kavaratti Island. The maximum wind directional and temporal change was observed during this season owing to the fact that the transition period indicates wind flow pattern reversal. The AP was approaching towards higher pressure and winds were observed more north-northeasterly. During 9-12 November 2009, the tropical cyclone Phyan was also experienced. During Phyan, passage wind was predominantly in a south/south-west direction and wind speed and AP recorded at Kavaratti Island were ~16 ms⁻¹ and ~998 hPa respectively, which resulted in a sea surge of ~10 cm e.g.,².

Conclusion

The present study is intended to provide insight into the evolution process of the mean meteorological parameters at Kavaratti Island. Measurements at Kavaratti Island indicate that the wind flow in this region was predominantly north/north-westerly. The only exception was in June-July during which west/south-westerly wind flow was observed. It was interesting to note that southerly wind flow was totally absent in this region throughout the year.

The atmospheric pressure in the Lakshadweep Island region reveals slow monthly variability in which the minimum (~1000 hPa) occurs during May-June and the maximum (~1012 hPa) during December-January. Apart from the diurnal day-night variability, the relative humidity which was normally in the range ~60-85%, increased to ~70-95% during southwest monsoon. The AT in the Kavaratti Island showed a progressively increasing trend from January to May in which diurnal day-night variability was a regular feature. With onset of the southwest monsoon, the AT dropped to ~26°C and remained around same until August. By September, AT increased to ~28°C and remained more or less steady around this level for the rest of the year. However, intermittent drops in AT were observed due to the northeast monsoon rainfall. During the cyclone Phyan, wind gust and AP recorded by the NIO-AWS were over 13 ms⁻¹ and ~997 hPa respectively. Wind was predominantly in a south/south-west direction accompanied by intense rainfall which resulted in atmospheric cooling. The AT had dipped to 25°C and RH has increased to ~94%.

Acknowledgements

Authors are thankful to the Director, CSIR-National Institute of Oceanography, Goa for providing necessary infrastructure to carry out the above work. Thanks are also due to Dr. M.S. Sayed Ismail Koya, Director, Department of Science & Technology Lakshadweep Islands for his constant support and encouragement throughout the study period. The above study was carried out under the funds provided by the Lakshadweep Development Corporation Ltd., Cochin, India. This is CSIR-NIO contribution No. 5626.

References

- 1 R.G. Prabhudesai, Antony Joseph, Yogesh Agarwadekar, Prakash Mehra, Vijay Kumar, and Ryan Luis, Integrated Coastal Observation Network (ICON) for real-time monitoring of sea-level, sea-state, and surface-meteorological data, *proc. symp. OCEANS (2010)*, 1-9
- 2 Joseph, Antony R.G. Prabhudesai, Prakash Mehra, V. Sanil Kumar, K.V. Radha Krishnan, Vijay Kumar, K. Ashok Kumar Yogesh Agarwadekar, U.G. Bhat, Ryan Luis, Pradhan Rivankar, and Blossom Viegas, Response of west India coastal regions and Kavaratti lagoon to the November 2009 tropical cyclone Phyan, *Natural Hazards* 57 2(2011) 293-312

- 3 Hubert, W. E, Morford, D. R., Hull. A. N., and R. E. Englebretson., Forecasters Handbook for the Middle East/Arabian Sea, *United States Naval Environmental Prediction Research Facility* ,(1983) 1-226.
- 4 Roa, Y. P., South West Monsoon, *Meteorological monograph synoptic. Meteorology No. 1/1979* (1979) 1-387.
- 5 G. J. Haltiner and F. L. Martin., Dynamical and physical meteorology, *Quarterly Journal of the Royal Meteorological Society*, 84 (1957) 304-305.
- 6 Bradley, F. and Fairall C., A guide to making climate quality meteorological and flux measurements at sea, NOAA Technical Memorandum PSD-311, *National Oceanic and Atmospheric Administration, Office of Oceanic and Atmospheric Research, Earth System Research Laboratory, Colorado*, (2006) pp 1-109.
- 7 Raymond, W. H., Estimating moisture profiles using a modified power law, *Journal of Applied Meteorology* 39 (2000) 1059-1070.
- 8 Gadgil, S., The Indian monsoon and its variability, *Annual Review of Earth and Planetary, Sciences*, 31 (2003) 429-467.
- 9 Srinivasan, V. and Ramamurthy, K., Forecasting manual, (North-East Monsoon) part 4, *India Meteorological Department, Poona, FMU Report No. IV-18.4 (1073)* pp1-180.
- 10 Ramesh Kumar, M. R., Sankar, S, and Reason, C, An investigation into the conditions leading to monsoon onset over Kerala. *Theoretical and Applied Climatology*, 95(2009). 69-82.
- 11 Pearce, R. P. and Mohanty, U.C., Onsets of the summer Monsoon 1979-198, *Journal of Atmos Science*, 41 (1984) 1620-1639.